Protein Unfolding in Detergents: Effect of Micelle Structure, Ionic Strength, pH, and Temperature

Daniel E. Otzen
Department of Life Sciences, Aalborg University, DK-9000 Aalborg, Denmark

ABSTRACT The 101-residue monomeric protein S6 unfolds in the anionic detergent sodium dodecyl sulfate (SDS) above the critical micelle concentration, with unfolding rates varying according to two different modes. Our group has proposed that spherical micelles lead to saturation kinetics in unfolding (mode 1), while cylindrical micelles prevalent at higher SDS concentrations induce a power-law dependent increase in the unfolding rate (mode 2). Here I investigate in more detail how micellar properties affect protein unfolding. High NaCl concentrations, which induce cylindrical micelles, favor mode 2. This is consistent with our model, though other effects such as electrostatic screening cannot be discounted. Furthermore, unfolding does not occur in mode 2 in the cationic detergent LTAB, which is unable to form cylindrical micelles. A strong retardation of unfolding occurs at higher LTAB concentrations, possibly due to the formation of dead-end protein-detergent complexes. A similar, albeit much weaker, effect is seen in SDS in the absence of salt. Chymotrypsin inhibitor 2 exhibits the same modes of unfolding in SDS as S6, indicating that this type of protein unfolding is not specific for S6. The unfolding process in mode 1 has an activation barrier similar in magnitude to that in water, while the activation barrier in mode 2 is strongly concentration-dependent. The strong pH-dependence of unfolding in SDS and LTAB suggests that the rate of unfolding in anionic detergent is modulated by repulsion between detergent headgroups and anionic side chains, while cationic side chains modulate unfolding rates in cationic detergents.

INTRODUCTION

Ionic detergents, such as sodium dodecyl sulfate (SDS), bind to most proteins with high affinity (Reynolds et al., 1967; Decker and Foster, 1966; Ikai, 1976). The interactions are governed by the aggregation state of the detergent. While monomeric detergents bind to the native state as conventional ligands, that is, they bind to a small number of sites in a saturable manner (Reynolds and Tanford, 1970; Yonath et al., 1977; Bordbar et al., 1997), micelles act as denaturants. Thus global protein unfolding typically occurs above the critical micelle concentration (cmc), which for SDS is ~7 mM in water (Reynolds et al., 1967; Jones et al., 1975; Turro et al., 1995; Gimel and Brown, 1996). The ability to denature proteins stems from the amphiphilic properties shared by protein and detergent. For example, SDS binds to proteins via interactions between the sulfate group and positively charged amino acid side chains, and between the alkyl chain and hydrophobic side chains (Wang et al., 1996; Yonath et al., 1977). The enthalpy of binding of SDS monomers to cationic sites in the native state of lysozyme is exothermic, and contributes −2.5 kcal/mol/residue (Jones and Manley, 1979). SDS-denatured proteins retain a large degree of ordered, albeit non-native, structure, but little is known of the mechanism(s) by which unfolding occurs. Our group has previously characterized two different interaction modes between SDS micelles and proteins, based on the kinetics of SDS-mediated unfolding of the model protein S6, a 101-residue monomeric mixed α-helix/β-sheet protein from the small ribosomal subunit of the prokaryote *Thermus thermophilus* (Otzen and Oliveberg, 2002a). Unfolding of S6 requires the presence of micelles because the relaxation phase associated with denaturation is only observed above the cmc of SDS. Below the cmc, binding of SDS is slow and multiphasic and leads to an increase in fluorescence, rather than a decrease, consistent with the binding of monomeric SDS to S6. Our discussion has therefore been focused on the interaction between protein and micelles. We showed that SDS unfolds S6 by two different unfolding routes, and hypothesized that these routes were linked to changes in micellar structure. In both unfolding routes, the binding of SDS micelles appears to lead to an initial expansion of the protein to form a partially denatured state before the major unfolding transition. Between 1 and 600 mM SDS, the average micellar aggregation number grows essentially linearly from 63 to 91, shifting the dominant population structure from spherical toward more elongated cylindrical micelles (Croonen et al., 1983; Clint, 1992). In our model, spherical micelles lead to simple ligand-binding-type unfolding kinetics, while cylindrical micelles unfold proteins by a power-law dependence. The concentration-dependence in mode 2 may arise because higher [SDS] leads to more cylindrical micelles, which are able to wrap themselves plastically around the protein and bind progressively more tightly in the transition state. Based on protein engineering data, we have proposed a minimalist unfolding model, where SDS micelles attacks and distorts the native state N, forming a partially disrupted state before the major unfolding transition (Otzen and Oliveberg, 2002a).

Submitted May 10, 2002, and accepted for publication June 14, 2002.

Address reprint requests to Daniel E. Otzen, Department of Life Sciences, Aalborg University, Sohngaardsholmsvej 49, DK-9000 Aalborg, Denmark. Tel.: +45 96 35 85 25; Fax: +45 98 14 18 08; E-mail: dao@bio.auc.dk.

0006-3495/02/10/2219/12 $2.00

Here I investigate the effect of micellar structure, electrostatic effects, and activation barriers on detergent-mediated unfolding in more detail. To test our hypothesis on the correlation between unfolding modes and micellar structure, I have altered the ionic strength of the solution by increasing the concentration of NaCl. High ionic strength screens the repulsion between the sulfate headgroups, lowering the concentration at which cylindrical micelles start to form (Jönsson et al., 1998). Increasing [NaCl] should therefore lead to an earlier onset of mode 2 unfolding. I have also examined unfolding in the cationic detergent lauryl trimethyl ammonium bromide (LTAB), which does not form cylindrical micelles (Malliaris et al., 1986), and therefore should not lead to mode 2 unfolding at all. In both cases, the results are consistent with our hypothesis. In addition, I report that the unfolding rate decreases at intermediate SDS concentrations and high LTAB concentrations; a possible explanation for this could be an excluded volume effect. The existence of multiple protein unfolding modes in SDS is not specific for S6, as I also observe them in the 64-residue mixed α-helix/β-sheet protein chymotrypsin inhibitor 2 (CI2) from barley.

The activation enthalpy of unfolding in SDS in the two modes is examined. Unfolding in water takes place from the native state, rather than an expanded state as in SDS, and this might be expected to alter the activation barrier. However, the activation barrier in mode 1 is very similar to that in water, suggesting that there is only a small enthalpic difference between the native state and the expanded ground state in SDS. In mode 2, the activation barrier is [SDS]-dependent, and decreases markedly between 100 and 600 mM. This agrees with the notion that longer SDS-micelles are better at stabilizing the transition state and thus reducing the energy barrier.

In addition to altering micellar structure, changes in ionic strength will probably also affect the protein-detergent interaction. To focus on the electrostatics of protein-detergent interactions at constant ionic strength, I have measured unfolding rates between pH 4 and 11. Over this pH range the total charge of the ionizable side chains on the protein will vary significantly. I find a strong pH-dependence on unfolding rates that is not correlated to protein pI, but rather to titration of acidic (in SDS) and basic (in LTAB) side chains. The pK_a values of the side chains are shifted by ~2 pH units relative to water, most likely due to the local increase in proton concentration at the micellar surface.

Note that because this work is based on kinetic unfolding data, I only discuss the steps between the ground state of unfolding (the expanded micelle-bound state) and the rate-limiting transition state for unfolding. The kinetic studies do not give direct information on the end-state of the reaction, viz., the denatured protein in complex with detergent. It is not unlikely that several rapid conformational changes follow the transition state, but it is not possible to monitor them under the present experimental conditions.

MATERIALS AND METHODS

Lauryl trimethylammonium chloride (LTAB) and lauryl trimethylammonium chloride (LTAC) were from FeF A/S (Koege, Denmark). All other chemicals were from Sigma-Aldrich Corp. (St. Louis, MO). S6 and CI2 were purified as described (Otzen et al., 1999b; Jackson et al., 1993).

Stopped-flow unfolding kinetics were carried out as described (Otzen and Oliveberg, 2002a). Briefly, protein was mixed with detergent in a 1:5 ratio to give a final protein concentration of 0.5 μM. The reaction was monitored by following the change in fluorescence of the proteins' single tryptophan residue, and the time profiles were fitted to single exponentials with drift to obtain the unfolding rate constant k_{obs}. For measuring kinetics at different pH values the following buffers were used at a concentration of 25 mM, all with 20 mM Na^+ (in addition to the Na^+ counterion in SDS): pH 4 and 5, NaOAc; pH 6, MES; pH 7, HEPES; pH 8, Tris; pH 9 and 10, Tris (SDS) or Gly (LTAB). The experiments at different ionic strengths (0–0.4M NaCl) were carried out using 25 mM Tris, pH 8.

Data analysis

Unfolding kinetics can be grouped in three different modes, namely modes 1, 2, and 0.

Mode 1

At moderate salt concentrations (20–60 mM NaCl), the rate constant for unfolding increases steeply with SDS concentration, and then stabilizes at a plateau around 100 mM SDS. This behavior can be described by a minimal scheme involving rapid binding (complete within the dead-time of stopped-flow mixing, ~5 ms) and subsequent global unfolding.

$$\mathrm{P} + \mathrm{SDS} \overset{K_1}{\rightleftharpoons} \mathrm{P^*{:}SDS} \xrightarrow{k_{unf}^{mode\ 1}} \mathrm{P{:}SDS^{Mode\ 1}}$$

Scheme 1

Mode 2

Above ~200 mM SDS at moderate salt concentrations, the unfolding rate constant increases markedly in a manner that is linear in a double-logarithmic plot. We have presented evidence that this can also be described by rapid binding followed by unfolding (Otzen and Oliveberg, 2002a). This leads to two different unfolding regimes in SDS:

$$\begin{array}{l} \overset{K_1}{\rightleftharpoons}\ \mathrm{P^*{:}SDS} \xrightarrow{k_{unf}^{mode\ 1}} \mathrm{P{:}SDS^{Mode\ 1}} \\ \mathrm{P} + \mathrm{SDS} \\ \overset{K_2}{\rightleftharpoons}\ \mathrm{P^*{:}SDS} \xrightarrow{k_{unf}^{mode\ 2}} \mathrm{P{:}SDS^{Mode\ 2}} \end{array}$$

Scheme 2

Unfolding in mode 1 and 2 in SDS are analyzed according to the following equation (Otzen and Oliveberg, 2002a):

$$k_{obs} = \frac{k_{unf}^{mode\ 1}}{1 + 1/K_1([SDS]_{total} - cmc_p)} + k^{0.5M\ SDS}\left[\frac{[SDS]_{total} - cmc_p}{0.5M - cmc_p}\right]^{\Delta n}. \quad (1)$$

The first term in the equation refers to unfolding in mode 1 (hyperbolic [SDS]-dependence), the second to mode 2 (power-law [SDS] dependence). K_1 is an association constant between SDS micelles and proteins, $k_{unf}^{mode\ 1}$ is the plateau-level rate constant of unfolding at low SDS concentrations (<100 mM), and $k^{0.5M\ SDS}$ is the rate constant of unfolding at 0.5 M SDS in mode 2. Δn can be interpreted as the increase in the number of protein-SDS interactions formed during the unfolding step in mode 2. Because no denaturation is observed below cmc, the value for [SDS] is replaced by ($[SDS]_{total} - cmc_p$) in Eq. 1, where cmc_p is the cmc value of SDS in the presence of the protein. The free detergent concentration is safely approximated by the total detergent concentration, as detergent is present in great excess over protein. Even at the lowest SDS concentration used (2 mM), the ratio of SDS micelles to protein molecules is above 40, assuming a micellar aggregate number of 50 (Jönsson et al., 1998).

Mode 0

In the absence of NaCl, there is a decline in unfolding rate constants at intermediate SDS concentrations before the onset of mode 2 unfolding. A minimalistic way to model this is to invoke the binding of additional detergent molecules to the protein complex P*: SDS (analogous to uncompetitive inhibition in enzyme catalysis), rather than to the unbound protein P (which would correspond to competitive inhibition). Formation of a dead-end complex between free P and SDS would not lead to a decline in unfolding rates at high detergent concentrations. In the model, the dead-end complex SDS:P*:SDS forms with an association constant K_{inh}, which is smaller than K_1:

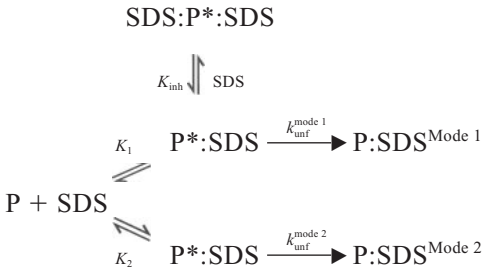

Scheme 3

For simplicity, I assume that there is no difference between the detergent micelles that bind to P and to P*:SDS and that only one micelle binds to P*:SDS. This means that the micellar concentration in both binding steps is described by the term ($[SDS]_{total} - cmc_p$) in terms of monomers, leading to the following equation:

$$k_{obs} = \frac{k_{unf}^{mode\ 1}}{1 + 1/K_1([SDS]_{total} - cmc_p) + K_{inh}([SDS]_{total} - cmc_p)} + k^{0.5M\ SDS}\left[\frac{[SDS]_{total} - cmc_p}{0.5M - cmc_p}\right]^{\Delta n}. \quad (2)$$

If, however, it is assumed that two micelles bind to P*SDS, the new term introduced into Eq. 2 has to be modified to K_{inh}*($[SDS]total - cmc_p)^2$, which decreases the quality of the fits (data not shown). Note that the data do not allow a rigorous conclusion about the stoichiometry of the dead-end complex; I merely attempt to present a possible model. The details of the model do not have a bearing on the discussion, but serve to emphasize the complexity of protein unfolding in detergent.

Cationic detergents

Unfolding rates in the cationic detergents LTAB and LTAC are modeled according to the following scheme:

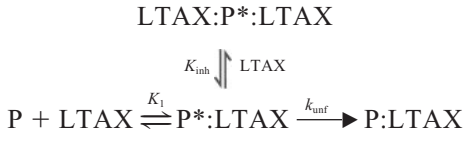

Scheme 4

Here LTAX represents LTAB or LTAC. The data are fitted to the following equation:

$$k_{obs} = \frac{k_{unf}}{1 + 1/K_1([LTAX] - cmc_p) + K_{inh}([LTAX] - cmc_p)}. \quad (3)$$

Again it is assumed that the micelles binding to free P and P*:LTAX are similar and that one micelle binds in each case. This is supported by the deterioration in the quality of the fits upon including other stoichiometries (data not shown).

Because of the pronounced inhibition during unfolding in LTAB, unrestrained fitting of the kinetic data using Eq. 3 led to unrealistically high values of k_{unf} and large errors associated with them. Therefore, k_{unf} was defined as twice the highest ordinate value of the fitted plot (without any associated error). k_{unf} was then locked to this value and the fitting was repeated to obtain values for K_1, cmc, and K_{inh}. While this locking is an arbitrary decision, the absolute value of k_{unf} is not central to this study. I later compare values of k_{unf} for a large number of mutants, but assume that any systematic deviation between the locked value and the actual value will be overall similar for the different mutants.

Unfolding rates at different temperatures were fitted to the following equation:

$$\log\left(\frac{k}{T}\right) = \frac{\ln(3356)}{\ln(10)} + \frac{\Delta S_u^{\ddagger}}{\ln(10) * R} - \frac{\Delta H_u^{\ddagger}}{\ln(10) * RT}. \quad (4)$$

Here $\Delta S_u^{\ddagger}$ and $\Delta H_u^{\ddagger}$ are the activation entropy and enthalpy of unfolding, respectively. The term for vibrational frequency (k_BT/h, around 10^{13} s^{-1}), which is conventionally used in the analysis of simple chemical reactions (Fersht, 1998), has been replaced with the factor $3356T$ (which is 10^6 s^{-1} at 298 K). This figure constant represents the fastest step in protein folding, namely closing of a loop (Hagen et al., 1996). The factor only affects the absolute value of the entropy of activation.

RESULTS

The influence of ionic strength on unfolding kinetics

In 20 mM NaCl at pH 8, S6 shows only two distinct unfolding modes between 1 and 600 mM SDS (Fig. 1 *A*, Scheme 2). Below 100 mM SDS, the rate of unfolding (k_{unf}) reaches a plateau (mode 1), but it starts to rise steeply above 100–200 mM, according to a power-law relationship (mode 2). These relationships, summarized in Scheme 2, are described in more detail in Materials and Methods. Changing the salt concentration profoundly affects the unfolding profile. In the complete absence of Na^+ ions (except those associated with lauryl sulfate as counterions), an additional mode (mode 0) is visible, manifesting itself as a decline in unfolding rates at intermediate detergent concentrations (Fig. 1 *A*). This is tentatively modeled as the formation of a dead-end complex between the protein complex and additional SDS micelles (Scheme 3). Mode 0 was not mentioned in our previous report (Otzen and Oliveberg, 2002a), because it is absent at the salt concentration (20 mM NaCl) used for all experiments in that study. Mode 0 disappears above 10 mM NaCl, whereas mode 1 fades away above 150 mM, so that only mode 2 is observed around 300–400 mM NaCl (Fig. 1 *B*, Table 1). I have included unfolding rate constants for the protein CI2 at pH 8 in 20 mM NaCl (Fig. 1 *A*) to show that the occurrence of these three modes is not limited to S6.

The NaCl concentration at which mode 1 disappears may be estimated more accurately using a plot of [SDS]* versus $\sqrt{I}$. [SDS]* is the SDS concentration where the unfolding rates in modes 1 and 2 are equal (calculated from Eq. 1), while I is the ionic strength (the electrostatic screening effect of NaCl is proportional to $\sqrt{I}$). The plot fits satisfactorily ($r = 0.98$) to a straight line that extrapolates to [SDS]* = 0 at $\sqrt{I} = 13.3$ $\sqrt{\text{mM}}$ (Fig. 1 *C*), showing that mode 1 completely disappears around 177 mM NaCl.

Altering the ionic strength not only affects the distribution of unfolding modes; the log of the unfolding rate constant in mode 2 interpolated to 0.5 M SDS ($k_{unf}^{0.5M\ SDS}$) increases linearly with $\sqrt{I}$, while the log of the unfolding rate constant in mode 1 ($k_{unf}^{mode\ 1}$) decreases linearly with $\sqrt{I}$ (Fig. 1 *D*). For comparison I include the effect of NaCl on the rate constant of unfolding of the S6 mutant Val→Ala-6/Leu→Ala-30 in the denaturant urea (wild-type S6 is so stable that it does not unfold in urea). In addition, Δn decreases linearly with $\sqrt{I}$ (Fig. 1 *E*).

Unfolding in cationic detergent does not occur via mode 2, probably due to a simpler micelle structure

S6 also unfolds in the cationic detergent LTAB, leading to a decline in fluorescence. LTAB's cmc is much higher than that of SDS (10 mM vs. 2 mM in 20 mM NaCl), and unfolding is only observed above 10 mM LTAB. There are two major differences compared to unfolding in SDS: 1) no mode 2 unfolding is seen in LTAB (Fig. 2 *A*). The high level of absorption of the Br^- counterion in the near UV range restricts measurements to at most 125 mM LTAB. However, measurements up to 0.76 M in the less strongly absorbing detergent LTAC (where Br^- is replaced with Cl^-) show no increase in unfolding rates at high detergent concentrations. This is entirely in accord with LTAB's and LTAC's inability to form cylindrical micelles. 2) There is a pronounced decrease in unfolding rates above ~20 mM LTAB. The decrease is unlikely to be caused by a stabilization of the native state due to the increasing concentration of detergent counterions; Cl^- and Br^- only stabilize proteins to a small extent (Baldwin, 1996). Changes in micellar structure cannot be invoked either. The decline is reminiscent of the decrease at intermediate SDS concentrations at low ionic strength and below pH 8 (Fig. 1 *A*). Thus, a minimalistic kinetic explanation could be the formation of a dead-end complex LTAB:P*:LTAB between the protein and LTAB with a smaller association constant than K_1 (Scheme 4 and Eq. 3). The kinetic parameters are summarized in Table 2.

To examine the characteristics of this putative dead-end complex, I have determined K_1 and K_{inh} for 22 mutants of S6 in which large hydrophobic side chains buried in the core of the protein have been substituted for Ala (Table 3). These mutations lead to significant changes in the thermodynamic stability and unfolding rates in water compared to wild-type (Otzen and Oliveberg, 2002b). However, for both K_1 and K_{inh} I find no correlation with the mutants' physical properties, such as thermodynamic stability, unfolding rates in water, or change in hydrophobicity (estimated from Kyte-Doolittle analysis). There is, however, a reasonable correlation between K_1 and K_{inh}; a linear fit yields a correlation coefficient of 0.75 with a slope of 0.29 ± 0.05 and an intercept of 0.006 ± 0.014 (Fig. 2 *B*). Thus, both parameters appear to be linked to the properties of the protein. This supports the view that the inhibition of unfolding in mode 0 arises from a genuine protein-detergent interaction rather than a change in the physical properties of the detergent.

In general, cationic amphiphiles bind cooperatively to most proteins to form complexes similar to those formed by SDS, but with diminished affinity (Nozaki et al., 1974). The reason for this difference has been suggested to be the side chains involved. Favorable electrostatic interactions for cationic amphiphiles are Glu and Asp, which only have two and one methylene side chain groups, whereas the corresponding side chains for anionic amphiphiles are Lys and Arg with four and three methylene groups; this makes a significant hydrophobic contribution to binding as well as a favorable electrostatic interaction (Tanford, 1991). This may explain why RNase A (Jones et al., 1973) and CI2 (data not shown) are resistant to LTAB-denaturation.

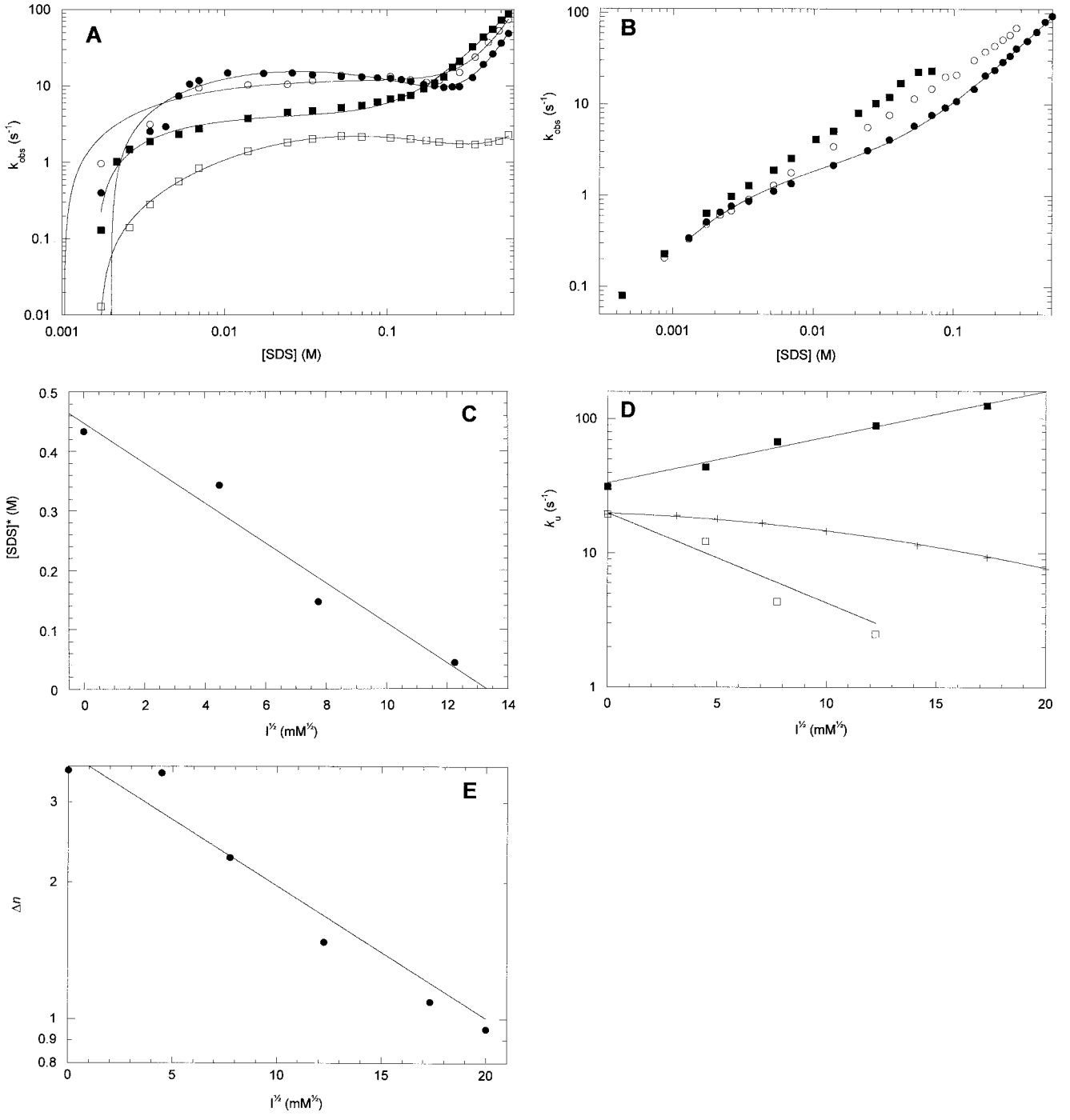

FIGURE 1 Effect of exogenous Na^+ (added as NaCl) on the different SDS-interaction modes at pH 8. (*A*) 0 mM (●), 20 mM (○), and 60 mM (■) Na^+. For comparison, unfolding rates for CI2 in 20 mM NaCl (□) are included. Data for 20 and 60 mM (mode 1 and 2) are fitted to Eq. 1 and those for 0 mM NaCl and for CI2 (modes 1, 2, and 0) are fitted to Eq. 2. (*B*) 150 mM (●), 300 mM (○), and 400 mM (■) Na^+. Data for 150 mM are fitted to Eq. 1. (*C*) [SDS]*, the SDS concentration at which the unfolding rates in modes 1 and 2 are equal, plotted versus the square root of the ionic strength. The linear fit (correlation coefficient $R = 0.98$) intersects the x axis at $\sqrt{I} = 13.3$ $\sqrt{}$mM. (*D*) Dependence of the fast (■) and slow (□) unfolding rates on the square root of the ionic strength. Also included are the rates of unfolding of the destabilized S6 mutant Val→Ala-6/Leu→Ala-30 in 6.6 M urea as a function of ionic strength (+). To facilitate comparison with the unfolding rates in SDS, the unfolding rates in urea are multiplied by a factor of 33. (*E*) Dependence of the cooperativity of unfolding of the fast phase (the Δn-value in Eq. 2) on the square root of the ionic strength.

TABLE 1 Kinetic parameters for unfolding of S6 in SDS at 25°C and pH 8 in different concentrations of NaCl

[NaCl] (M)	$k_{unf}^{Mode\ 1}$ (s^{-1})*	K_1 (M^{-1})†	$k^{0.5M\ SDS}$ (s^{-1})‡	Δn	cmc_p (mM)§	K_{inh} (M^{-1})¶
0‖	19.5 ± 1.4	364 ± 89	31.3 ± 0.8	3.53 ± 0.19	2.0 ± 0.2	64 ± 1.30
0.02**	12.3 ± 0.8	303 ± 115	43.8 ± 1.4	3.48 ± 0.22	1.7 ± 0.2	—
0.06**	4.34 ± 0.46	445 ± 305	67.6 ± 0.7	2.27 ± 0.05	1.0 ± 0.4	—
0.15**	2.49 ± 1.18	177 ± 359	88.9 ± 1.2	1.48 ± 0.04	0.5 ± 0.4	—
0.3††	—	—	125.2 ± 2.6	1.09 ± 0.02		—
0.4††	—	—	162 ± 20	0.95 ± 0.05		—

*The unfolding rate in mode 1 at plateau level.
†The association constant between SDS micelles and free protein.
‡The unfolding rate in mode 2 interpolated to 0.5 M SDS.
§The cmc value of SDS in the presence of S6 at the given NaCl concentration and 25 mM Tris-Cl pH 8.
¶The inhibition constant between SDS micelles and the P*:SDS complex (Scheme 3).
‖Data at this NaCl concentration fitted to Eq. 2 (encompassing modes 1, 2, and 0).
**Data at this NaCl concentration fitted to Eq. 1 (encompassing modes 1 and 2).
††Data at this NaCl concentration fitted to the second term in Eq. 1 (encompassing mode 2 only).

Temperature-dependence of the two unfolding routes

The rate constants for S6′ two unfolding processes are highly temperature-dependent. The Eyring plots (log k_{unf}/T vs. $1/T$) for unfolding rates in modes 1 and 2 are linear within the accessible temperature range (15–45°C) (Fig. 3 *A*). The unfolding rate in mode 2 is shown at three different SDS concentrations because of the strong variation of unfolding rates with SDS concentration in this mode. Deviations from linearity in Eyring plots are generally attributed to changes in the heat capacity of the system, e.g., through binding of water molecules upon exposure of hitherto buried protein surface area (Oliveberg et al., 1995). The linear plots in Fig. 3 *A* indicate that there is no significant heat capacity change between the ground state and transition state for unfolding in SDS.

Values for $\Delta H_u^{\ddagger}$ and $\Delta S_u^{\ddagger}$ in mode 1 and 2, calculated from data in Fig. 3 *A* using Eq. 4, are shown in Table 4. For comparison, I include the corresponding values for unfolding in water (based on unfolding rates in GdmCl that have been extrapolated to 0 M denaturant at different temperatures). Unfolding in water represents a simple transition between the native state and the transition state of unfolding (Otzen et al., 1999b). Note that the latter process is accompanied by a significant change in heat capacity, since the Eyring plot is distinctly curved (Fig. 3 *A*).

pH-dependence of unfolding in SDS and LTAB

Unfolding rates in SDS (mode 1) decrease dramatically with increasing pH in a titratable fashion with an apparent pK_a value of ~5.4 (Fig. 4 *A*). The pH-dependence of the unfolding rates in SDS cannot be explained by changes in protein stability over this pH range. The stability of wild-type S6 between pH 4 and 10 is so high that it does not denature below 100°C; however, CD thermal scans of a destabilized mutant of S6 (Leu→Ala-79) under the same buffer conditions as the detergent experiments indicate no change in denaturation temperature (90°C) over the pH range 4–10 (data not shown). S6 has no His residues and

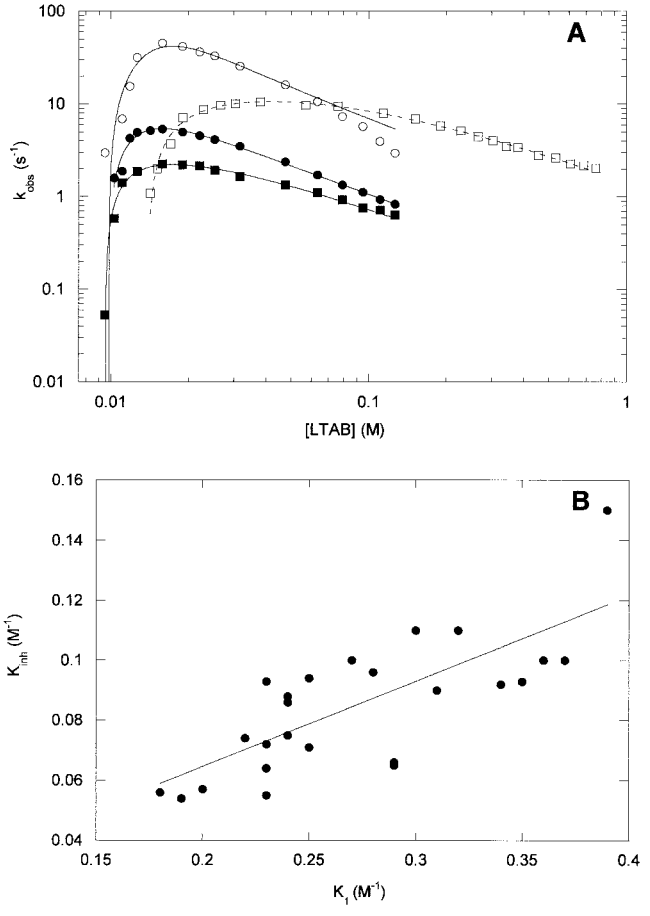

FIGURE 2 (*A*) Unfolding of S6 in LTAB at pH 7 (■), pH 9 (●), and pH 10 (○) and in LTAC at pH 7 (□). Also shown are the best fits to Eq. 3. (*B*) Correlation between K_1 and K_{inh} for 22 different mutants of S6. The mutations involve truncation of hydrophobic side chains to Ala in the protein's core (Table 3). The linear fit yields a correlation coefficient of 0.75 with a slope of 0.29 ± 0.05 and an intercept of 0.006 ± 0.014.

TABLE 2 Kinetic parameters for unfolding of S6 in LTAB and LTAC at 25°C and pH 7

Detergent	k_{unf} (s^{-1})*	K_1 (M^{-1})†	cmc (mM)‡	K_{inh} (M^{-1})§
LTAB	4.44	259 ± 18	9.48 ± 0.08	59.7 ± 2.7
LTAC	16.7	125 ± 18	13.9 ± 0.2	10.6 ± 1.0

*The unfolding rate (Scheme 4).
†The association constant between LTAX micelles and free protein.
‡The cmc value of SDS in the presence of S6 at the given NaCl concentration and 25 mM Tris-Cl pH 8.
§The inhibition constant between LTAX micelles and the P*:LTAX complex.

therefore no side chains that titrate between pH 4 and 8 in an aqueous environment.

Could the overall charge on the protein govern the pH-dependence for unfolding in SDS? Wild-type S6 has a p*I* of 6.55. To test the effect of changes in p*I*, I examined the behavior of two mutants, Glu→Ala-41/Glu→Ile-42 and Arg→Met-46/Arg→Val-47, in which the p*I* has been shifted to 9.0 and 5.0, respectively, without decreasing the thermodynamic stability of the protein appreciably (data not shown). Yet in both SDS and LTAB, these mutants manifested the same pH-dependence as S6 wild-type with pK_a values around 5.4 (Fig. 4, *A* and *B*). This rules out the involvement of p*I*.

Unfolding rates in LTAB present a mirror-image to those in SDS, increasing strongly above pH 7, although titration is not complete at pH 11 (Fig. 4 *B*). Measurements were limited to pH 11 and below, as the stability of S6 decreases significantly above pH 11, giving rise to an increase in unfolding rates that will perturb measurements of the intrinsic unfolding rate in detergent (data not shown).

TABLE 3 Kinetic parameters for the unfolding of S6 wild-type and 21 hydrophobic deletion mutants in LTAB at 25°C and pH 9

Mutant	k_{unf} (s^{-1})*	K_1 (M^{-1})†	K_{inh} (M^{-1})‡
Wild-type S6	10.7	340	92.0
Tyr → Ala-4	51.7	250	71.0
Val → Ala-6	67.2	290	66.0
Val → Ala-9	19.0	230	64.0
Leu → Ala-19	85.7	310	90.0
Leu → Ala-21	14.9	240	88.0
Ile → Ala-25	3.64	240	75.0
Ile → Ala-26	117	360	100
Leu → Ala-30	107	330	100
Tyr → Ala-33	7.36	220	74.0
Ala → Gly-35	35.5	270	100
Val → Ala-37	2467	390	150
Ile → Ala-48	15.7	250	94.0
Phe → Ala-60	57.2	230	93.0
Val → Ala-65	109.6	300	110
Met → Ala-67	118.0	280	96.0
Leu → Ala-75	34.0	240	86.0
Leu → Ala-79	371.9	290	65.0
Val → Ala-88	28.1	190	54.0
Val → Ala-90	66.2	200	57.0

All errors ~10%.
*The unfolding rate (Scheme 4).
†The association constant between LTAB micelles and free protein.
‡The inhibition constant between LTAB micelles and the P*:LTAB complex.

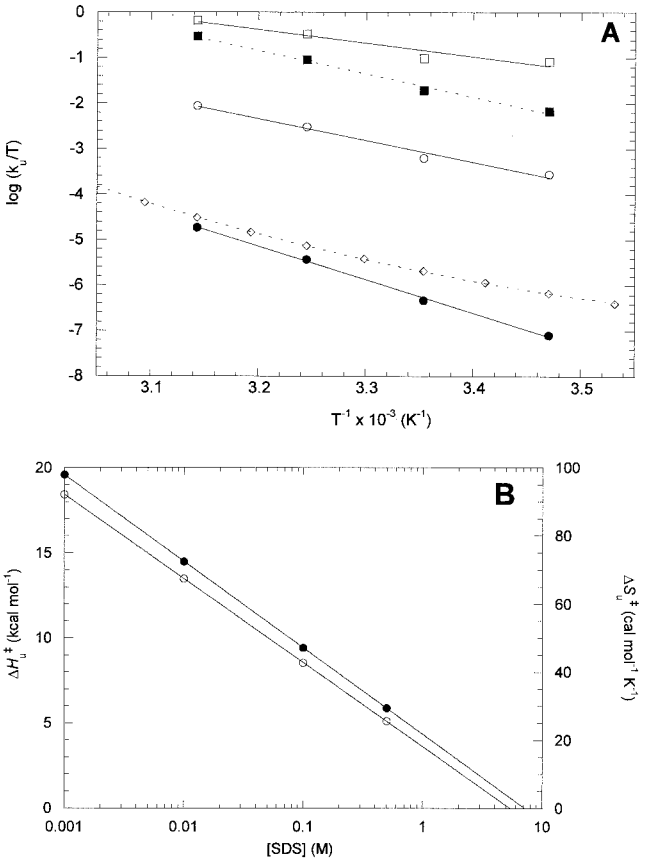

FIGURE 3 Eyring plots for $k_{unf}^{mode\ 1}$ (■) and unfolding rate constants in mode 2 at 10 (●), 100 (○), and 500 (□) mM SDS (mode 2) over the temperature interval 15–45°C. For comparison, the rates of unfolding of S6 in water, extrapolated from unfolding rates in GdmCl, are also shown (◇). (*B*) Dependence of the activation enthalpy of unfolding $\Delta H_u^{\ddagger}$ (●) and $\Delta S_u^{\ddagger}$ (○) for the fast unfolding phase on [SDS].

DISCUSSION

Ionic strength has a complex influence on protein unfolding in SDS

The observations on the effect of ionic strength on the unfolding rates in SDS are consistent with our hypothesis that the cylindrical micelles, which are the dominant species above 200 mM NaCl, are responsible for mode 2 unfolding. However, kinetic data can never prove specific models. While it is documented that high ionic strength favors the formation of cylindrical micelles (Jönsson et al., 1998), the effect of ionic strength on our protein-detergent system is complex, and models other

TABLE 4 Thermodynamic parameters for unfolding of S6 in SDS modes 1 and 2

Mode	$\Delta S_u^{\ddagger}$ (cal mol^{-1} K^{-1})*	$\Delta H_u^{\ddagger}$ (kcal/mol)†
1‡	54.9 ± 3.6	23.4 ± 1.4
2 (10 mM SDS)	67.5 ± 2.7	14.5 ± 0.4
2 (100 mM SDS)	42.8 ± 4.8	9.4 ± 0.9
2 (500 mM SDS)	25.6 ± 5.6	5.9 ± 1.2
Water§	38.6 ± 3.8	24.1 ± 1.1

*Based on the linear fits in Fig. 3 *A* to Eq. 4, where the intercept is $\ln(3356)/\ln(10) + \Delta S_u^{\ddagger}/(\ln(10)*R)$.

†Based on the linear fits in Fig. 3 *A* in Eq. 4, where the slope is $\Delta H_u^{\ddagger}/(\ln(10)*R)$.

‡k_{unf} in mode 1 is a plateau value and therefore not linked to a specific SDS concentration.

§Data for unfolding of S6 in water shown for comparison. Unfolding rates in water are extrapolated from unfolding rates in GdmCl at different temperatures (D. E. Otzen, unpublished observations).

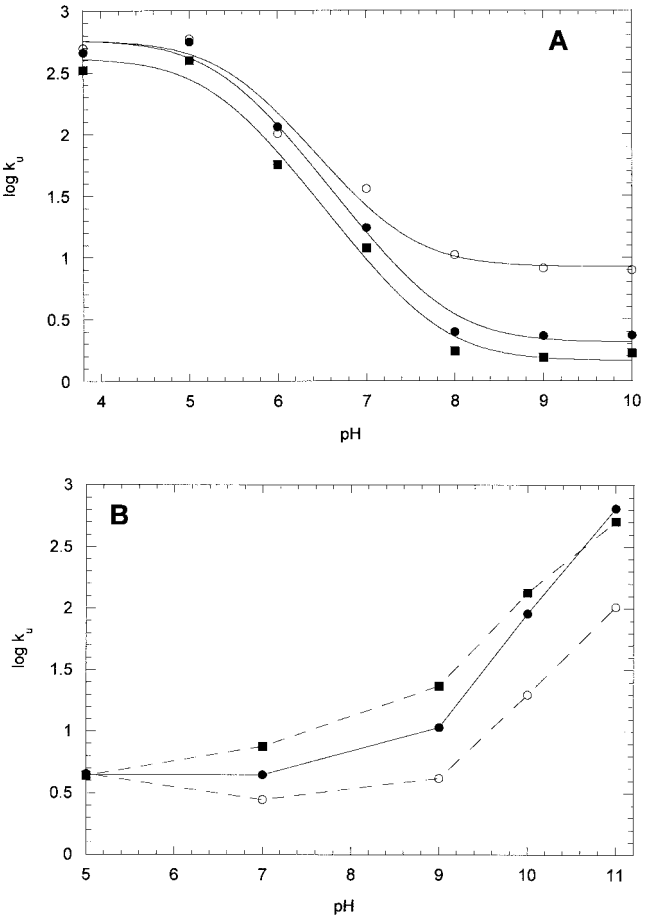

FIGURE 4 pH-dependence of the unfolding rate in mode 1 (k_u) in (*A*) SDS and (*B*) LTAB for wild-type S6 (●), EA41/EI42 (○), and RM46/RV47 (■). Data in (*A*) are fitted to a simple titration model between two protonation states with different unfolding rates in SDS. Although the three proteins have very different pI-values (5.0–9.0), $k_{unf}^{mode\ 1}$ titrates at pH 5.39 ± 0.16, 5.51 ± 0.20, and 5.31 ± 0.18, respectively, in SDS; in LTAB they also titrate in parallel, but titration is not complete within the measured pH-range.

than the bimodal unfolding scheme may also explain my observations. In addition to screening the repulsion between sulfate headgroups, increased ionic strength will have other effects.

First, it could alter the structure of the protein-micelle complex. High concentrations of inorganic salts, such as NaCl, favor compact protein conformations because they are excluded from the protein surface (Timasheff, 1993, 1998). Increasing concentrations of NaCl could gradually shift the conformation of the initial protein-detergent complex or the transition state toward more compact and structured states with kinetic properties that vary in distinct ways with SDS concentration. The main argument against this phenomenon playing a major role is that the excluded volume effect is weak for NaCl and only manifests itself strongly at concentrations in the molar range, well above the range at which my experiments have been carried out (Timasheff, 1993, 1998).

Second, high ionic strength could screen the electrostatic interactions between micelles and proteins. This interaction could be attractive or repulsive. Because protonation of negatively charged side chains appears to increase the kinetics of unfolding dramatically (see below), repulsion between the negative micellar charges and the negative charges on S6 seems to be the rate-limiting electrostatic component in unfolding. Therefore, increasing ionic strength should screen repulsion between S6 and SDS micelles, favoring binding and subsequent unfolding. There is some evidence in favor of this. The logarithm of the rate constant in mode 2 increases linearly with $\sqrt{I}$ as one might expect from an electrostatic screening effect (Fig. 1 *D*). The logarithm of the rate constant in mode 1 also changes linearly with $\sqrt{I}$; however, it decreases, rather than increasing. This decrease might be explained preferential stabilization by NaCl of the native state (as opposed to the protein-detergent complex discussed above), leading to an increase in the activation barrier to unfolding (Timasheff, 1993, 1998). Again, the main argument against stabilization of the native state is that the effect is not sufficiently strong. I have tried to quantitate the effect of NaCl on the kinetic stability of S6. Wild-type S6 can only be unfolded in guanidinium chloride (GdmCl), which is a salt. However, the destabilized mutant Val→Ala-6/LA30 can be unfolded in the nonionic denaturant urea, and its unfolding rate k_{unf} at different NaCl concentrations only declines by ~15% over the same range where $k_{unf}^{mode\ 1}$ decreases 7-fold (Fig. 1 *D*). [The urea-unfolding plot shows curvature because at low ionic strength the screening effect of NaCl ($\propto\sqrt{I}$) dominates, whereas at higher ionic strength the general salt-stabilizing effect ($\propto I$) takes over. SDS itself contributes a constant amount to *I* at the different NaCl concentrations, so inclusion of the SDS in the total *I* will by and large only shift all the $k_{unf}^{mode\ 1}$ points by the same degree to the

right.] Therefore salt-stabilization per se cannot explain the pronounced decline in unfolding rate in mode 1. It is possible that a complex interaction between SDS and NaCl may enhance the stabilizing effect of salt at relatively low SDS concentrations (below 0.1 M). This point is discussed further in the section on unfolding in cationic detergent.

There is also a clear reverse correlation between Δn and $\sqrt{I}$ (Fig. 1 *E*). We have tentatively interpreted Δn as the increase in protein-SDS interactions that occurs during unfolding in mode 2 (Otzen and Oliveberg, 2002a). From this it follows that a smaller number of new interactions are made during unfolding at higher salt concentrations. A minimalist explanation could be that the burst-phase state formed before the major unfolding step (Otzen and Oliveberg, 2002a) binds a larger number of detergent molecules at higher NaCl concentrations (because the micelles increase in size), leading to a smaller number of accessible binding sites for the subsequent unfolding step.

Because of the major role played by electrostatic repulsion (see below), it is not surprising that screening the charges at high ionic strength (0.4 M NaCl) accelerates unfolding. However, while mode 2 unfolding rates in SDS in 0.4 M NaCl (where the screening effect is close to saturation) are 6-fold higher than in the absence of exogenous Na^+ (162 vs. 31 s^{-1}), it is less than a third of the value of $k_{unf}^{mode\ 1}$ measured at pH 5 (around 540 s^{-1}). This shows that even very high screening cannot compensate entirely for repulsive charges.

The thermodynamics of unfolding in SDS

Between 15 and 45°C, the aggregation number in low salt changes from ~50 to ~30 (Jönsson et al., 1998). It cannot be ruled out that this will contribute to $\Delta H_u^{\ddagger}$ in both unfolding modes. However, the variation in aggregation number with temperature is complex, and could skew the Eyring plot. The good fits in Fig. 3 *A* suggest that this does not affect the thermodynamics of unfolding significantly.

The activation enthalpies of unfolding in mode 1 and in water are strongly endothermic and similar in value (~24 kcal/mol). The cooperativity of unfolding for the fast unfolding process (the Δn value in Eq. 1) decreases linearly with temperature ($R = 0.99$ for 4 points, data not shown). This means that unfolding rates at different SDS concentrations do not increase to the same extent with temperature. As a consequence, $\Delta H_u^{\ddagger}$ for mode 2 is markedly dependent on SDS concentration. Between 1 and 500 mM SDS, it changes from 19.6 ± 0.3 to 5.9 ± 1.2 kcal/mol, following a linear dependence on log[SDS] (Fig. 3 *B* and Table 4). The linear correlation extrapolates to 0 kcal/mol in activation energy around 8 M SDS, but this extrapolation is entirely hypothetical, because SDS undergoes additional phase changes around 1 M and has a solubility limit well below 8 M (Jönsson et al., 1998).

We have previously suggested that the concentration-dependence in mode 2 unfolding arises because higher [SDS] leads to more cylindrical micelles, which are able to wrap themselves plastically around the protein in the transition state. The longer the micelles get, the tighter they bind in the transition state, leading to a greater stabilization relative to the ground state (Otzen and Oliveberg, 2002a). This makes it reasonable that $\Delta H_u^{\ddagger}$ in mode 2 should decrease with concentration.

Though different interactions are broken and made on going to the transition states for unfolding in detergent versus water, unfolding in SDS (mode 1) and in water lead to remarkably similar (endothermic) changes in enthalpy. This may be fortuitous. It is not expected a priori, as the SDS-unfolding pathway appears to involve an unfolding intermediate N* (Otzen and Oliveberg, 2002a), which is not observed in GdmCl-mediated unfolding of S6 wild-type (Otzen et al., 1999b). Therefore, the activation barrier to unfolding in SDS lies between the transition state and the preceding N*, whereas it lies between the transition state and the native state (N) in water. $\Delta H_u^{\ddagger}$ for an elementary reaction will always be positive because energy is required to create the partially formed bonds of the transition state. However, in more complex reactions such as the conformational changes involved in protein unfolding, enthalpy changes can occur at many different levels. It is illustrative to make an inventory of the interactions made and broken during the activation energy of unfolding. The following interactions contribute to $\Delta H_u^{\ddagger}$. 1) Loss of van der Waals interactions and hydrogen bonds in N* or N (positive); 2) formation of new interactions between the protein and water, as well as the removal of steric clashes (negative); 3) formation of new interactions between protein and SDS or GdmCl (negative); 4) loss of water-water interactions (positive); and 5) loss of SDS/GdmCl interactions (positive for SDS, probably negligible for GdmCl).

The interactions in (3) and (5) are clearly different in SDS versus water. Also, the interactions in (2) and (4) are expected to be different in SDS versus GdmCl, as SDS and GdmCl will affect water activity and the structure of the transition state to different extents.

The coincidence of the activation enthalpies could arise either from cancellation of differences in (2)–(5) or from the fact that (1) dominates and N* and N have similar enthalpies. If the latter is the case, it suggests a remarkable parallel between unfolding under different circumstances, implying that essentially the same interactions have to be broken whether unfolding from the native state in GdmCl or the more expanded state in SDS, so that there is only a small enthalpic difference between the native state and the expanded ground state in SDS.

The measured entropy change reflects the increase in entropy from the liberation of water upon unfolding and the increased conformational freedom of the protein, as well as the decrease in entropy from increased binding of SDS (or

GdmCl) to the transition state. The $\Delta S_u^{\ddagger}$-values listed in Table 4 also vary significantly with SDS concentration in mode 2, in a way that parallels $\Delta H_u^{\ddagger}$ (Fig. 3 *B*). Note that the absolute value of $\Delta S_u^{\ddagger}$ is garnered with uncertainty. According to classical transition state theory, maximum activation values are based on the fastest possible breaking of chemical bonds (Fersht, 1998), but protein unfolding is a much more complex process involving conformational changes that are significantly slower. Although I have attempted to compensate for this using current estimates for the fastest possible events in protein folding (Hagen et al., 1996), the values must remain tentative.

The apparent entropy-enthalpy compensation between $\Delta S_u^{\ddagger}$ and $\Delta H_u^{\ddagger}$ is a phenomenon that has also been observed in other contexts, such as ionic and non-ionic surfactants in various liquids (Kresheck, 1975). However, this will not be discussed further, because closer analysis suggests that the linear relationship is an artifact of the linkage between entropy and enthalpy evident in Eq. 4 (Cornish-Bowden, 2002).

The pH-dependence of unfolding rates reflects perturbed pK_a values

It is obvious that the p*I* of the protein does not influence the pH-dependence of the unfolding rates in SDS. The apparent pK_a of 5.4 for unfolding in SDS is more likely to reflect the specific titration of ionizable side chains. The most likely candidates are the carboxylic acid groups of Glu and Asp, whose pK_a values, ~pH 3.5–4 in water, will be altered in other environments. For example, Glu and Asp residues in a 20-residue helix peptide had pK_a values shifted to 4.9–5.4 in SDS and dodecylphosphocholine micelles (Wang et al., 1996), while the peptide carboxylic acid group pK_a at membrane interfaces is estimated to be ~5.7 (Wimley and White, 1996). There are several ways in which the pK_a values of Glu and Asp can be shifted in the micellar environment. First, the negative charge on the sulfate groups concentrates protons in their vicinity to an extent that has been estimated to increase the proton concentration at the micellar surface by 1–2 orders of magnitude, leading to a local drop in pH relative to bulk solution (O'Neil and Sykes, 1989; Van der Goot et al., 1991). Second, pK_a values will be altered in an environment such as the micelle interior, which alters the equilibrium between the ionized and non-ionized species, here the carboxylate ion versus the neutral carboxylic acid group. Both effects will lead to an upward shift in pK_a, the first one because it decreases the effective pH, the second because it favors the non-ionized species because the burial of an unpaired charge in a nonpolar environment is very unfavorable (Fersht et al., 1985). The location of the carboxyl groups in the micelle (surface or interior) will determine which of the two effects plays the dominant role. Assuming that Glu and Asp on average lie close to the micelle surface, it is possible to calculate the expected pK_a shifts using the quantitative approach of Fromherz (Fromherz, 1989). In charged micelles, the total pK_a-shift relative to water ΔpK_{mw} can be split up into the intrinsic pK_a-shift ΔpK_i (i.e., the change in free energy necessary to transfer the acid and conjugate base from water into the micellar environment) and the electrostatic potential contribution; that is, the shift in "local pH" due to the electrostatic potential Ψ as follows:

$$\Delta pK_{mw} = \Delta pK_i - (F\Psi/2.3 * RT). \quad (5)$$

where *F* is Faraday's constant. The assumption that ΔpK_i is similar in charged and uncharged micellar interfaces is supported by other experimental data (Fromherz, 1989). In SDS micelles Ψ is estimated to be around ~−134 mV (Fromherz, 1989), which gives an electrostatic contribution of ~2.3 pH units. In other words, the local increase in proton concentration on the SDS micellar surface is enough to explain the pK_a shift. If the carboxyl groups were to penetrate into the micelle interior, the pK_a could be perturbed to an even larger extent. Carboxyl group pK_a values can shift by up to 5 units when a side chain is fixed in an apolar environment because this favors the uncharged state (Urry et al., 1994). This suggests that the Glu and Asp side chains are mainly in contact with the negatively charged micellar surface, rather than being sequestered in the apolar micellar interior or somewhere in between. Structural studies on SDS-protein complexes, such as those underlying the "protein-decorated micelle structure" model (Ibel et al., 1990), indicate that hydrophilic side chains do not interact directly with the hydrophobic interior of micelles, but can be associated with the anionic headgroup. Analogously, it is common for amphipathic peptides to lie parallel to the membrane surface rather than penetrate it (Hunt et al., 1997). A complicating factor in these considerations is, however, that the organization of SDS micelles around the protein could change as the Glu and Asp side chains protonate and thus become more hydrophobic (though still strongly polar).

In LTAB, the pH-dependence of the unfolding step is likely to be determined by the protonation of Lys, Arg, and Tyr, which titrate over different ranges, but the limited data do not permit us to distinguish different deprotonation steps. However, the pK_a values of these side chains are shifted downward in LTAB, using arguments analogous to those for SDS. For example, the cationic detergent CTAB (with a C_{16} tail rather than a C_{12} tail, as for LTAB) has an electrostatic potential Ψ of +148 mV (Fromherz, 1989), which is expected to lead to a downward shift in pK_a of 2.5 pH units.

The data thus suggest that while cationic side chains are good binding sites for SDS on the protein surface (Yonath et al., 1977; Jones and Manley, 1979, 1980; Wang et al., 1996), the kinetics of interaction with SDS are modulated by the repulsion between the sulfate groups and the protein's anionic side chains (and, conversely, between

LTAB's quaternary ammonium's group and cationic side chains). The introduction or removal of negatively charged side chains also had profound effects on the rate of unfolding of the cellulase Cel-45 in the anionic detergent LAS, which could be interpreted in the light of a simple electrostatic interaction model (Otzen et al., 1999a). The denaturing properties of SDS and other charged detergents are linked to repulsions between different detergent micelles bound to the protein surface. Thus, electrostatic repulsions play a central role in protein-detergent interactions. Electrostatic repulsions also affect the stability of proteins in the absence of detergent. The native state of barnase is probably more destabilized by such repulsions than the denatured and transition states (Oliveberg et al., 1994; Oliveberg and Fersht, 1996), as seen by the rapid increase in unfolding rates at decreasing pH. Similar observations have been made for other proteins (Negin and Carbeck, 2002).

I gratefully acknowledge support from EMBO and the Danish Technical Science Research Council, as well as constructive discussions with Drs. Alfred Holtzer and Mikael Oliveberg.

REFERENCES

Baldwin, R. L. 1996. How Hofmeister ion interactions affect protein stability. *Biophys. J.* 71:2056–2063.

Bordbar, A. K., A. A. Saboury, M. R. Housaindokht, and A. A. Moosavi-Movahedi. 1997. Statistical effects of the binding of ionic surfactant to protein. *J. Colloid Interface Sci.* 192:415–419.

Clint, J. H. 1992. Surfactant Aggregation. Chapman and Hall, New York.

Cornish-Bowden, A. 2002. Enthalpy-entropy compensation: a phantom phenomenon. *J. Biosci.* 27:121–126.

Croonen, Y., E. Geladé, M. Van der Zegel, M. Van der Auweraer, H. Vandendriessche, F. C. De Schryver, and M. Almgren. 1983. Influence of salt, detergent concentration and temperature on the fluorescence quenching of 1-methylpyrene in sodium dodecyl sulfate with m-dicyanobenzene. *J. Phys. Chem.* 87:1426–1431.

Decker, R. V., and J. F. Foster. 1966. The interaction of bovine plasma albumin with detergent anions. Stoichiometry and mechanism of binding of alkylbenzenesulfonates. *Biochemistry.* 5:1242–1249.

Fersht, A. R. 1998. Structure and Mechanism in Protein Science. A Guide to Enzyme Catalysis and Protein Folding. Freeman and Co., New York.

Fersht, A. R., J. P. Shi, J. Knill-Jones, D. M. Lowe, A. J. Wilkinson, D. M. Blow, P. Brick, P. Carter, M. M. Y. Wae, and G. Winter. 1985. Hydrogen bonding and biological specificity analyzed by protein engineering. *Nature.* 314:235–238.

Fromherz, P. 1989. Lipid coumarin dye as a probe of interfacial electrical potential in biomembranes. *Methods Enzymol.* 171:376–387.

Gimel, J. C., and W. Brown. 1996. A light-scattering investigation of the sodium dodecyl sulfate-lysozyme system. *J. Chem. Phys.* 104: 8112–8117.

Hagen, S. J., J. Hofrichter, A. Szabo, and W. A. Eaton. 1996. Diffusion-limited contact formation in unfolded cytochrome c: estimating the maximum rate of protein folding. *Proc. Natl. Acad. Sci. U. S. A.* 93:11615–11617.

Hunt, J. F., T. N. Earnest, O. Bousché, K. Kalghatgi, K. Reilly, C. Horváth, K. J. Rothschild, and D. M. Engelman. 1997. A biophysical study of integral membrane protein folding. *Biochemistry.* 36:15156–15176.

Ibel, K., R. P. May, K. Kirschner, H. Szadkowski, E. Mascher, and P. Lundahl. 1990. Protein-decorated micelle structure of sodium-dodecylsulfate-protein complexes as determined by neutron scattering. *Eur. J. Biochem.* 190:311–318.

Ikai, A. 1976. Stepwise degradation of serum low density lipoprotein by sodium dodecyl sulfate. *J. Biochem.* 29:679–688.

Jackson, S. E., M. Moracci, N. elMasry, C. M. Johnson, and A. R. Fersht. 1993. Effect of cavity-creating mutations in the hydrophobic core of chymotrypsin inhibitor 2. *Biochemistry.* 32:11259–11269.

Jones, M. N., and P. Manley. 1979. Binding of *n*-alkyl sulphates to lysozyme in aqueous solution. *J. Chem. Soc. Faraday Trans.* 75: 1736–1744.

Jones, M. N., and P. Manley. 1980. Interaction between lysozyme and *n*-alkyl sulfates in aqueous solution. *J. Chem. Soc. Faraday. Trans.* 76:654–664.

Jones, M. N., H. A. Skinner, and E. Tipping. 1975. The interaction between bovine serum albumin and surfactants. *Biochem. J.* 147:229–234.

Jones, M. N., H. A. Skinner, E. Tipping, and A. Wilkinson. 1973. The interaction between ribonuclease A and surfactants. *Biochem. J.* 135: 231–236.

Jönsson, B., B. Lindman, K. Holmberg, and B. Kronberg. 1998. Surfactants and polymers in aqueous solutions. Wiley and Sons, New York.

Kresheck, G. C. 1975. Surfactants in Water: A Comprehensive Treatise. F. Franks, editor. Plenum Press, New York. 95–167.

Malliaris, A., J. Lang, and R. Zana. 1986. Micellar aggregation numbers at high surfactant concentration. *J. Colloid Interface Sci.* 110:237–241.

Negin, R. S., and J. D. Carbeck. 2002. Measurement of electrostatic interactions in protein folding with the use of protein charge ladders. *J. Am. Chem. Soc.* 124:2911–2916.

Nozaki, Y., J. A. Reynolds, and C. Tanford. 1974. The interaction of a cationic detergent with bovine serum albumin and other proteins. *J. Biol. Chem.* 249:4452–4457.

Oliveberg, M., and A. R. Fersht. 1996. Formation of electrostatic interactions in the protein-folding pathway. *Biochemistry.* 35:2726–2737.

Oliveberg, M., Y. J. Tan, and A. R. Fersht. 1995. Negative activation enthalpy in the kinetics of protein folding. *Proc. Natl. Acad. Sci. U.S.A.* 92:8926–8929.

Oliveberg, M., S. Vuilleumier, and A. R. Fersht. 1994. Thermodynamic study of the acid denaturation of barnase and its dependence of ionic strength: evidence for residual electrostatic interactions in the acid/thermally denatured state. *Biochemistry.* 33:8826–8832.

O'Neil, J. D. J., and B. D. Sykes. 1989. NMR studies of the influence of dodecyl sulfate on the amide hydrogen exchange kinetics of a micelle-solubilized hydrophobic tripeptide. *Biochemistry.* 28:699–797.

Otzen, D. E., L. Christensen, and M. Schülein. 1999a. A comparative study of the unfolding of EGV in denaturant and surfactant. *Protein Sci.* 8:1878–1887.

Otzen, D. E., O. Kristensen, M. Proctor, and M. Oliveberg. 1999b. Structural changes in the transition state of protein folding: an alternative interpretation of curved chevron plots. *Biochemistry.* 38:6499–6511.

Otzen, D. E., and M. Oliveberg. 2002a. Burst-phase expansion of native protein prior to global unfolding in SDS. *J. Mol. Biol.* 315:1231–1240.

Otzen, D. E., and M. Oliveberg. 2002b. Conformational plasticity in folding of the split β-α-β protein S6: evidence for burst-phase disruption of the native state. *J. Mol. Biol.* 317:613–627.

Reynolds, J. A., S. Herbert, H. Polet, and J. Steinhardt. 1967. The binding of divers detergent anions to bovine serum albumin. *Biochemistry.* 6:937–943.

Reynolds, J. A., and C. Tanford. 1970. The gross conformation of protein-sodium dodecyl sulfate complexes. *J. Biol. Chem.* 245:5161–5165.

Tanford, C. 1991. The Hydrophobic Effect. Formation of Micelles and Biological Membranes. Wiley and Sons, New York.

Timasheff, S. N. 1993. The control of protein stability and association by weak interactions with water: how do solvents affect these processes? *Annu. Rev. Biophys. Biomol. Struct.* 22:67–97.

Timasheff, S. N. 1998. Control of protein stability and reactions by weakly interacting cosolvents: the simplicity of the complicated. *Adv. Protein Chem.* 51:355–432.

Turro, N. J., X.-G. Lei, K. P. Ananthapadmanabhan, and M. Aronson. 1995. Spectroscopic probe analysis of protein-surfactant interactions: the BSA/SDS system. *Langmuir.* 11:2525–2533.

Urry, D. W., S. Peng, D. C. Gowda, T. M. Parker, and R. D. Harris. 1994. Comparison of electrostatic- and hydrophobic-induced pKa shifts in polypentapeptides. The lysine residue. *Chem. Phys. Lett.* 225:97–103.

Van der Goot, F. G., J. M. Gonzalez-Manas, J. H. Lakey, and F. Pattus. 1991. A "molten-globule" membrane-insertion intermediate of the pore-forming domain of colicin A. *Nature.* 354:408–410.

Wang, G., W. D. Treleaven, and R. J. Cushley. 1996. Conformation of human serum apolipoprotein A-I(166–185) in the presence of sodium dodecyl sulfate or dodecylphosphocholine by ^{1}H-NMR and CD. Evidence for specific peptide-SDS interactions. *Biochim. Biophys. Acta.* 1301:174–184.

Wimley, W. C., and S. H. White. 1996. Experimentally determined hydrophobicity scale for proteins at membrane interfaces. *Nat. Struct. Biol.* 3:842–848.

Yonath, A., A. Podjarny, B. Honig, A. Sielecki, and W. Traub. 1977. Crystallographic studies of protein denaturation and renaturation. 2. Sodium dodecyl sulfate induced structural changes in triclinic lysozyme. *Biochemistry.* 16:1418–1424.